Bioorganic & Medicinal Chemistry Letters 24 (2014) 2477–2480

Contents lists available at ScienceDirect

Bioorganic & Medicinal Chemistry Letters

journal homepage: www.elsevier.com/locate/bmcl

Synthesis, characterization, and PK/PD studies of a series of spirocyclic pyranochromene BACE1 inhibitors

Matthew Volgraf [a,*], Lina Chan [a], Malcolm P. Huestis [a], Hans E. Purkey [a], Michael Burkard [b], Mary Geck Do [b], Julie Harris [b], Kevin W. Hunt [b], Xingrong Liu [a], Joseph P. Lyssikatos [a], Sumeet Rana [b], Allen A. Thomas [b], Guy P. A. Vigers [b], Michael Siu [a]

[a] Genentech Inc., 1 DNA Way, South San Francisco, CA 94080, United States
[b] Array BioPharma, 3200 Walnut Street, Boulder, CO 80301, United States

ARTICLE INFO

Article history:
Received 14 January 2014
Revised 1 April 2014
Accepted 4 April 2014
Available online 13 April 2014

Keywords:
BACE1 inhibitors
Structure-based ligand design
Alzheimer's disease

ABSTRACT

The development of 1,3,4,4a,5,10a-hexahydropyrano[3,4-*b*]chromene analogs as BACE1 inhibitors is described. Introduction of the spirocyclic pyranochromene scaffold yielded several advantages over previous generation cores, including increased potency, reduced efflux, and reduced CYP2D6 inhibition. Compound **13** (BACE1 IC_{50} = 110 nM) demonstrated a reduction in CSF Aβ in wild type rats after a single dose.

Alzheimer's disease is characterized by the deposition of beta amyloid (Aβ) plaques and neurofibrillary tangles in the brain, leading to neurodegeneration, dementia, and ultimately death.[1] The amyloid hypothesis holds that the primary causative agent of the disease is the Aβ peptide, either as soluble oligomers or aggregated fibers. As such, recent disease-modifying approaches have focused on reducing or eliminating these Aβ plaques.[2] One approach involves inhibiting the protease beta-site APP cleaving enzyme 1 (BACE1), which is responsible for the rate-limiting step during the formation of Aβ peptides.[3]

We have previously described spirocyclic BACE1 inhibitors based on chroman[4] and γ-oxa-pyranochromene scaffolds[5] (Fig. 1). The most potent compounds within these series contained spirocyclic acyl guanidines able to effectively engage the catalytic aspartates of the protease, yet inhibitors featuring this warhead invariably suffered from P-glycoprotein efflux ratios (P-gp ER) >3 (**1**, Fig. 1). It was found that the efflux ratios could be improved by lowering the TPSA of the warhead using an aminooxazoline-based warhead, albeit at the expense of BACE1 potency (**2** and **3**, Fig. 1).

In an effort to improve the potency of the spirocyclic pyranochromenes featuring aminooxazoline warheads, we sought to transpose the position of the A-ring oxygen to the δ-position relative to the spirocyclic center, which molecular modeling suggested might engage the N–H of a tryptophan residue (Trp76) in the BACE1 binding site (Fig. 1). We envisioned that by maintaining the same physicochemical property space as previous aminooxazolines, while simultaneously improving BACE1 potency, we might identify a compound suitable for benchmarking in our PK/PD assay measuring the reduction of CSF Aβ in wild type rats.

The presence of three contiguous chiral centers in the designs made the synthesis and subsequent control of diastereoselectivity a challenge within the δ-oxa-pyranochromene series. Employing a readily available chiral building block (D-xylose) enabled the synthesis of target compounds as single enantiomers (Scheme 1). Towards this end, enantiomerically pure dihydropyran **4**[6] was reduced in the presence of triethylsilane and boron trifluoride diethyl etherate to yield allylic acetate **5** in good yield. Following deacetylation, nucleophilic aromatic substitution cleanly provided ether **6**. Reduction of the nitrile to the aldehyde and conversion to the oxime provided key intermediate **7** which was primed for a [3+2] cycloaddition across the unactivated olefin. Following in situ formation of the nitrile oxide from the oxime using Koser's reagent,[7] isoxazole tetracycle **8** was formed in excellent overall yield. N—O bond cleavage[8] and imine hydrolysis provided alcohol **9** which could be deoxygenated using a two-step elimination/reduction protocol which also set the desired *trans*-ring junction of the pyranochromenone **10**. Tebbe olefination (→**11**) and

* Corresponding author. Tel.: +1 6504671305.
E-mail address: volgrafm@gene.com (M. Volgraf).

http://dx.doi.org/10.1016/j.bmcl.2014.04.012
0960-894X/

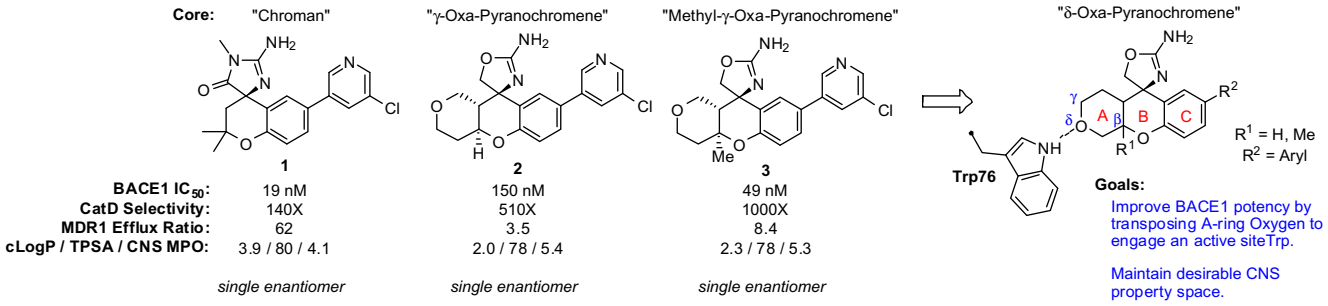

Figure 1. BACE1 lead compounds and strategy for further optimization.

formation of the spriocyclic aminooxazoline using literature conditions[9,10] provided advanced intermediate **12** as a 1:1 mixture of diastereomers about the spirocycle stereocenter. Suzuki cross-coupling and separation of the diastereomers provided the final targets **13**–**17** in enantiomerically pure form.

The new cores demonstrated improved BACE1 enzyme potency relative to the previously prepared spirocyclic pyranochromenes, with the 3-chloro-5-fluorophenyl **17** affording an IC_{50} value of 62 nM (Table 1). Chloropyridine **13** also performed well in the enzyme assay with an IC_{50} of 110 nM. However, the aminooxazolines remained much less potent than the acyl guanidines previously synthesized on the program. Given the high likelihood of P-gp efflux, acyl guanidines were not prepared with the new core.

A co-crystal structure of **13** with BACE1 confirmed our design hypothesis, demonstrating a unique water-bridged hydrogen bonding network between the A-ring oxygen atom and Trp76 (Fig. 2A, PDB code: 4PZW). The tricyclic pyranochromene core was oriented parallel to Tyr71, forming potentially favorable Van der Waals interactions with the BACE1 'flap' (Fig. 2B), while the chloropyridine occupied the S3 pocket of the protease. The aminooxazoline engaged the catalytic aspartates (Asp32 and Asp228) via hydrogen bonding and electrostatic interactions, similar to other aminooxazoline-based BACE1 inhibitors reported in the literature.[11]

The cellular potencies were generally found to be more potent than the enzyme IC_{50}, presumably due to the increased basicity of the aminooxazoline warhead relative to the acyl guanidines, resulting in accumulation of the more basic inhibitors in cellular compartments where BACE1 is also localized.[12] Meanwhile, selectivity against cathepsin D (CatD), a key off-target implicated in physiologically important roles, peaked at 180-fold.

The in vitro DMPK profile of the new series, specifically P-gp efflux ratios and predicted clearance in human liver microsomes (HLMs), was critical in prioritizing new compounds for PD evaluation (Table 1). The 3-chloro-5-fluorophenyl target **17** did not possess significant efflux (P-gp ER = 1.3), likely due to the increased lipophilicity ($cLogP$ = 3.3) and reduced polarity (TPSA = 66 Å) relative to the rest of the series. All other targets demonstrated P-gp efflux (P-gp ERs >3), indicating an increased likelihood of impaired brain exposure. Nevertheless, in vitro P-gp ERs were improved relative to the acyl guanidines previously described by our group.[4,5] Meanwhile, HLMs for the new series were predicted to be stable to moderately stable within the active stereochemical series (compounds **13**–**17**).

During the course of our synthetic efforts, we also synthesized the opposite A-ring *trans* stereoisomer of the pyranochromene core. It was found that the opposite *trans*-ring junction greatly impaired activity against BACE1, as observed in the comparison of matched pairs **13** (IC_{50} = 110 nM) and **18** (IC_{50} = 1.0 μM). Crystallography revealed the inability of this A-ring stereoisomer to engage Trp76 via a water-mediated hydrogen bond (Fig. 2C, PDB code: 4PZW) due to differences in A-ring conformation as well as

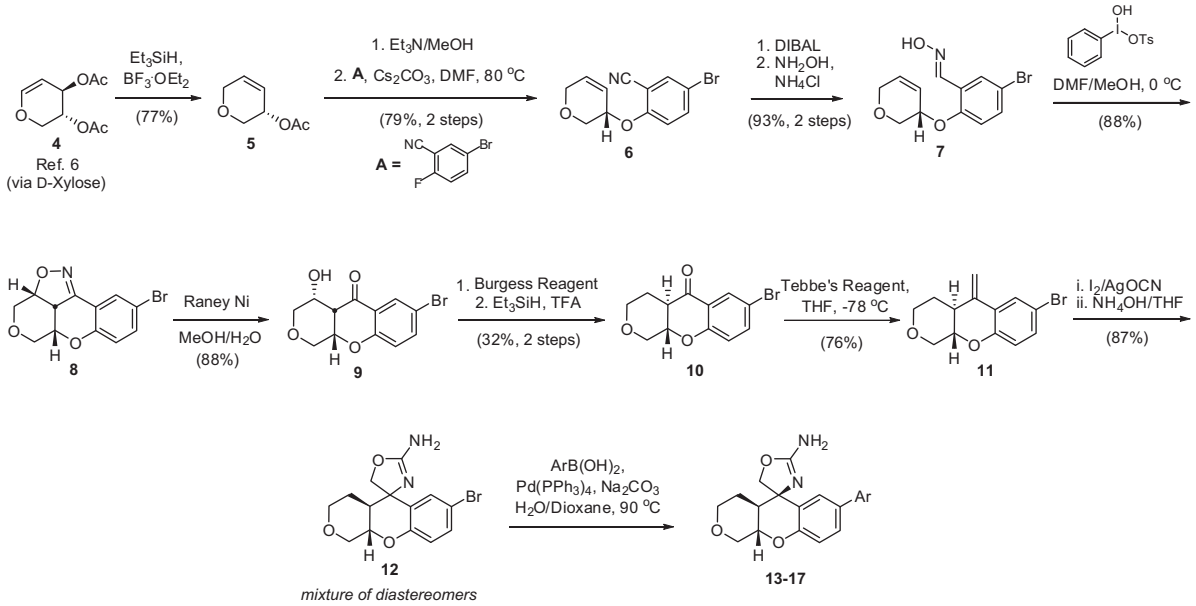

Scheme 1. Synthesis of δ-oxa-pyranochromene BACE1 inhibitors **13**–**17**.

Table 1
Physicochemical and pharmacological properties of γ-oxa-pyranochromene BACE1 inhibitors

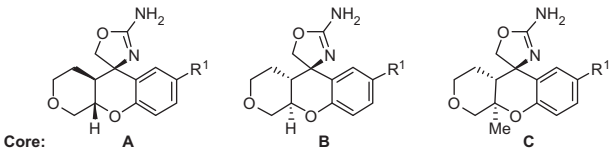

Compound	Core	R^1	*c*Log*P*/TPSA/CNS MPO[b]	BACE1 IC_{50}[c] (μM)	Cell IC_{50} APP^{WT}[d] (μM)	Enzyme/cell	CatD/BACE1	P_{app} (10^{-6} cm/s)	P-gp efflux ratio[e]	HLM[f] (mL/min/kg)
13	A	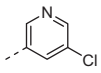	2.0/78/5.4	0.11	0.02	6.1	120	14	3.4	13
14	A	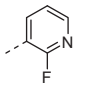	1.2/78/5.5	0.15	0.08	1.9	180	10	7.1	6
15	A	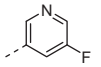	1.5/78/5.5	0.36	0.09	3.9	98	15	3.7	9
16	A	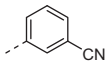	2.0/89/5.5	0.30	0.14	2.2	22	11	4.8	8
17	A	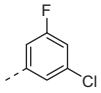	3.3/66/5.1	0.06	0.11	0.6	56	11	1.3	10
18	B	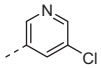	2.0/78/5.4	1.0	0.13	7.5	100	4.7	12	15
19	C[a]	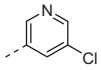	2.3/78/5.3	16	ND	ND	0.5	10	4.8	15

[a] Data for racemate.
[b] CNS MPO score calculated using an experimentally derived pK_a of 6.8 for compound **13**.
[c] Mean IC_{50} of at least two independent experiments.
[d] Mean IC_{50} of at least two independent experiments for cellular Aβ production.
[e] (B to A)/(A to B) value derived for compounds (1 μM) evaluated in LLC-PK1 cells transfected with human MDR1 (P-gp).
[f] Compounds (1 μM) incubated with human liver microsomes for 20 min at 37 °C in the presence of NADPH.
ND = not determined.

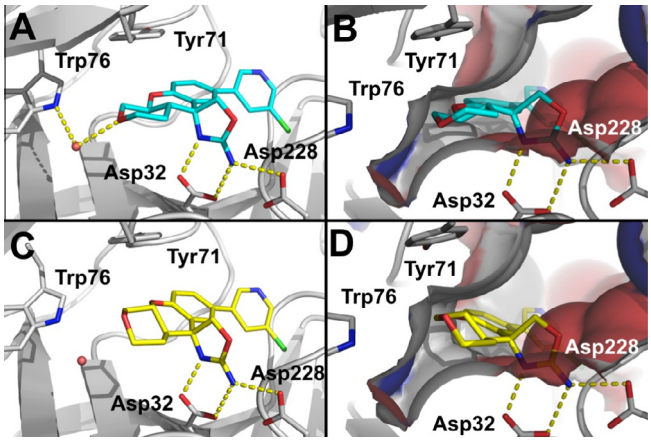

Figure 2. (A) Crystal structure of **13** bound to BACE1 active site (PDB code: 4PZW). (B) Surface rendering of BACE1 active site with **13** bound. (C) Crystal structure of **18** bound to BACE1 active site (PDB code: 4PZX). (D) Surface rendering of BACE1 active site with **18** bound.

a less favorable Van der Waals contacts with Tyr71 (Fig. 2D), accounting for the 10-fold loss in potency.

With these diastereomers in hand, we were surprised to discover a dramatic stereochemical dependence on CYP2D6 inhibition within the pyranochromene series. Serendipitously, the most potent stereoisomer did not inhibit CYP2D6 while the other 3 stereoisomers prepared all displayed potent CYP2D6 inhibition of <1 μM (Table 2). Taken together, this data suggests that CYP2D6 inhibition within this subseries is dependent on both core and spirocenter stereochemistry. This observation coincides with the well studied difference in CYP2D6 inhibition by the stereoisomers quinidine and quinine, illustrating the delicate interplay between stereochemistry and the 2D6 active site.[13]

We sought to improve the BACE1 enzyme potency of the δ-oxa-pyranochromene core via methyl substitution strategies. In the related γ-oxa-pyranochromene series, methyl substitution in the β-position relative to the spirocyclic center improved BACE1 potency and CatD selectivity (**2**→**3**, Fig. 1). Preparation of the matched pair **19** yielded a dramatic loss in potency (>16 μM). This loss in potency may be explained by the stereochemical preference of the pyranochromene A-ring observed between the two series (e.g. **13**: 110 nM vs **18**: 1.0 μM). In each case, the methyl group would occupy an opposite plane relative to the core in the active site.

We examined 3-chloropyridine **13** in a PD study comparing CSF Aβ in wild type rats with free brain concentrations of the inhibitor (Fig. 3). Analysis of the free brain/free plasma ratios of **13** at the 3 and 5 h timepoints after a 60 mg/kg dose were 0.45 and 0.29, respectively. Thus, despite predicted issues of P-gp efflux, brain/plasma ratios observed in vivo were acceptable. A 40% reduction in CSF Aβ was achieved after 3 h, with free brain concentrations of **13** reaching 250 nM, roughly 11-fold the cellular IC_{50} against

Table 2
Stereochemical dependence on CYP2D6 inhibition of γ-oxa-pyranochromene BACE1 inhibitors

	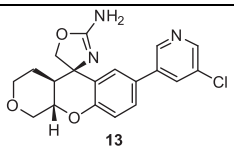 13	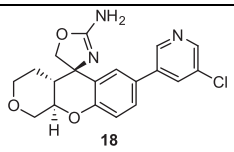 18	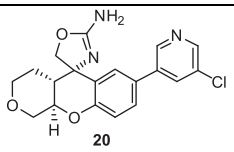 20	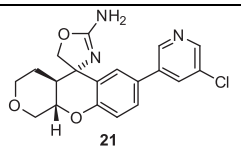 21
BACE1 IC_{50} (μM)[a]	0.11	1.0	7.7	17
CYP2D6 IC_{50} (μM)	>10	1.1	4.5	0.42

[a] Mean IC_{50} of at least two independent experiments.

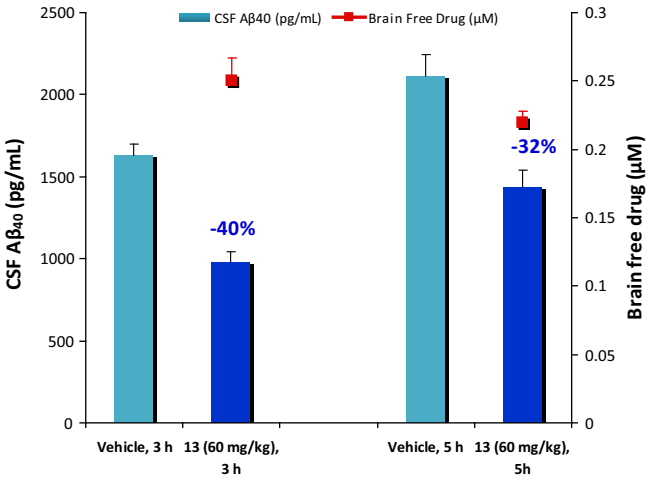

Figure 3. Rat pharmacodynamics of **13** ($Aβ_{1–40}$ lowering).

BACE1. The 5 h timepoint achieved 32% reduction with free brain concentrations roughly 10-fold over the cellular IC_{50}.

In summary, structure-based design was used to optimize the pyranochromene core of a series of BACE1 inhibitors. By transposing the position of an oxygen atom on the core to target a water-bridged hydrogen bond with an active site tryptophan, potency was improved while also maintaining physicochemical properties akin to marketed CNS drugs.[14] It was found that the relative configuration of the bicyclic ring system and the spirocyclic aminooxazoline was important for both BACE1 potency and CYP2D6 inhibition. Free brain concentrations of chloropyridine **13** in a PD-assay in wild type rat were in excess of the cellular IC_{50} by greater than 10-fold and achieved a maximal Aβ reduction in CSF of 40% after 3 h. Despite achieving acceptable observed free brain/free plasma ratios, the observed Aβ reduction was not sufficient to progress **13** beyond rat PD. Further work within the aminooxazoline series focused on continuing to improve enzyme potency and reducing P-gp efflux. The results of these efforts will be disclosed in subsequent publications.

Acknowledgments

The authors would like to thank Yanzhou Liu, Yutao Jiang, Chris Hamman, Mengling Wong and Michael Hayes for analytical and purification support and Melis Coraggio and Young G. Shin for bio-analytical support.

Supplementary data

Supplementary data associated with this article can be found, in the online version, at http://dx.doi.org/10.1016/j.bmcl.2014.04.012. These data include MOL files and InChiKeys of the most important compounds described in this article.

References and notes

1. Kakob-Roetne, R.; Jacobsen, H. *Angew. Chem., Int. Ed.* **2009**, *49*, 3030.
2. Karran, E.; Mercken, M. M.; De Strooper, B. *Nat. Rev. Drug Discov.* **2011**, *10*, 698.
3. De Strooper, B.; Vassar, R.; Golde, T. *Nat. Rev. Neurol.* **2010**, *6*, 99.
4. Hunt, K. W.; Cook, A. W.; Watts, R. J.; Clark, C. T.; Vigers, G.; Smith, D.; Metcalf, A. T.; Gunawardana, I. W.; Burkard, M.; Cox, A. A.; Geck Do, M. K.; Dutcher, D.; Thomas, A. A.; Rana, S.; Kallan, N. C.; DeLisle, R. K.; Rizzi, J. P.; Regal, K.; Sammond, D.; Groneberg, R.; Siu, M.; Purkey, H.; Lyssikatos, J. P.; Marlow, A.; Liu, X.; Tang, T. P. *J. Med. Chem.* **2013**, *56*, 3379.
5. Thomas, A. A.; Hunt, K. W.; Volgraf, M.; Watts, R. J.; Liu, X.; Vigers, G. P. A.; Smith, D.; Sammond, D.; Tang, T. P.; Rhodes, S. P.; Metcalf, A. T.; Brown, K. P.; Otten, J. N.; Burkard, M.; Cox, A. A.; Geck Do, M. K.; Dutcher, D.; Rana, S.; DeLisle, R. K.; Regal, K.; Wright, A. D.; Groneberg, R.; Scearce-Levie, K.; Siu, M.; Purkey, H. E.; Lyssikatos, J. P.; Gunawardana, I. W. *J. Med. Chem.* **2014**, *57*, 878.
6. Matsuo, K.; Shindo, M. *Tetrahedron* **2011**, *67*, 971.
7. Raihan, M. J.; Kavala, V.; Kuo, C.-W.; Raju, R.; Yao, C.-F. *Green Chem.* **2010**, *12*, 1090.
8. Kozikowski, A. P.; Adamczyk, M. *Tetrahedron Lett.* **1982**, *23*, 3123.
9. Wittekind, R. R.; Rosenau, J. D.; Poos, G. I. *J. Org. Chem.* **1961**, *26*, 444.
10. Hassner, A.; Lorber, M. E.; Heathcock, C. H. *J. Org. Chem.* **1967**, *32*, 540.
11. Huang, H.; La, D. S.; Cheng, A. C.; Whittington, D. A.; Patel, V. F.; Chen, K.; Dineen, T. A.; Epstein, O.; Graceffa, R.; Hickman, D.; Kiang, T.-H.; Louie, S.; Luo, Y.; Wahl, R. C.; Wen, P. H.; Wood, S.; Fremeau, R. T., Jr. *J. Med. Chem.* **2012**, *55*, 9156.
12. Hilpert, H.; Guba, W.; Woltering, T. J.; Wostl, W.; Pinard, E.; Mauser, H.; Mayweg, A. V.; Rogers-Evans, M.; Humm, R.; Krummenacher, D.; Muser, T.; Schnider, C.; Jacobsen, H.; Ozmen, L.; Bergadano, A.; Banner, D. W.; Hochstrasser, R.; Kuglstatter, A.; David-Pierson, P.; Fischer, H.; Polara, A.; Narquizian, R. *J. Med. Chem.* **2013**, *56*, 3980.
13. Hutzler, J. M.; Walker, G. S.; Wienkers, L. C. *Chem. Res. Toxicol.* **2003**, *16*, 450.
14. Wager, T. T.; Hou, X.; Verhoest, P. R.; Villalobos, A. *ACS Chem. Neurosci.* **2010**, *1*, 435.